Eur. Phys. J. Plus (2016) **131**: 137
DOI 10.1140/epjp/i2016-16137-0

THE EUROPEAN PHYSICAL JOURNAL PLUS

Regular Article

Binaries application around the collinear equilibrium points in the photogravitational CR3BP with bigger primary oblate

Jagadish Singh[a] and Tajudeen Oluwafemi Amuda[b]

Department of Mathematics, Faculty of Science, Ahmadu Bello University, P.M.B 2222 Sokoto Road, Samaru, Zaria-Nigeria

Received: 20 November 2015 / Revised: 3 March 2016
Published online: 6 May 2016 –

Abstract. This paper studies the collinear equilibrium points of the restricted three-body problem under the effects of the oblateness of the bigger primary and the radiation pressure of the smaller primary. Using a semi-analytical and numerical approach, the positions and linear stability of these points are investigated for the binary systems RXJ 0450.1-5856 and Nova Cen 1969 (Cen X-4), and found to be affected by the oblateness and radiation pressure. The collinear points remain unstable in the sense of Lyapunov.

1 Introduction

A degenerated case of the three-body problem is the restricted three-body problem (R3BP). It describes the motion of an infinitesimal mass (third body) moving under the gravitational effects of two finite masses, called primaries, which move in circular orbits around their common center of mass on account of their mutual gravitational attraction and the infinitesimal mass not influencing the motion of the primaries. Several scientists and astronomers [1–10] have considered the applications of the R3BP to the dynamics of the stellar and solar systems, lunar theory and planetary sciences. The solutions to the classical problem, which have been developed over the centuries from [11–17] and others, form the basis of the study of the dynamics of the celestial bodies from their work to the recent advances in flight dynamics. The approximate circular motion of the planets around the Sun and the small masses of asteroids and satellites of planets compared to the planets' masses, originally suggested the formulation of the circular restricted three-body problem (CR3BP). The CR3BP possesses five equilibrium points. Three of them are in a straight line, and are called the collinear equilibrium points, while the other two forms equilateral triangles with the primaries, and are called triangular equilibrium points.

Several studies [18–26] have been carried out on the collinear libration points of the circular/ or elliptic restricted three-body problem. The authors of [18] and [21] have shown that the inner collinear point can be stable under certain conditions while [25] studied the effect of photogravitational force and oblateness in the perturbed R3BP and analyzed 128 cases of its model. The authors of [27] have investigated the effects of triaxiality of the bigger primary bodies on the collinear libration points of some binary systems moving in elliptical orbits around their common center of mass. Recently, [28] studied the bifurcation of artificial halo orbits from the Lyapunov planar family of periodic orbits around the collinear libration points and their results show that Solar Radiation Pressure is indeed a relevant ingredient for the new dynamical system.

The authors of [29] formulated the photogravitational CR3BP when at least one of the interacting bodies is an intense emitter of radiation. In certain stellar dynamics problems when a star acts upon a particle in a cloud of gas and dust, the dominant factor is by no means gravity, but the repulsive force of the radiation pressure. Researchers like [30–35] have included the radiation pressure force in their studies.

The bodies in the R3BP assumes that the masses concerned are spherically symmetrical in homogenous layers, but it is found that celestial bodies, such as Saturn and Jupiter, are not perfect spheres [36]. Rotation in stars produces an equatorial bulge due to centrifugal force. As a result of the rapid rotation after the formation of Neutron stars, white and black dwarfs, they may be considered oblate. A neutron star on formation can rotate at a rate of nearly a thousand rotations per second [37]. The pulsar PSRB1937+21 spinning about 642 times a second and the pulsar

[a] e-mail: jgds2004@yahoo.com
[b] e-mail: teejaymath@gmail.com

PSRJ1748-422ad spinning 716 times a second are some of the swiftest spinning pulsar [38]. This motivated several researchers [39–43] to include oblateness of the primaries in their studies of the R3BP.

In considering the bigger primary as an oblate spheroid and the smaller one as a source of radiation, a different version of the problem came into existence. In this context, we consider close binary stars in which the bigger primary is a stellar remnant (a neutron star, a white dwarf, a black dwarf) with the smaller one a low-mass stellar companion. A white dwarf, also called a degenerate dwarf, is a highly evolved stellar remnant of a giant star that has blown away its outer layers as planetary nebulae. It is composed of electron degenerated matter with no internal heat sources; however, it gradually radiates its residual energy until it becomes a black dwarf. Such types of binaries are not scarce, as stars of different masses have different life spans [44]. Examples of these are low-mass X-ray binaries (LMXBs), pre-LMXBs, and soft X-ray transient. These are the best natural counterparts in the system under study, which provides test beds for this astrophysical problem [45]. This constitutes an excellent model for the research under investigation.

In this paper, our effort is geared towards investigating the effects produced by oblateness of the bigger primary and the radiation pressure of the smaller primary on the existence of collinear equilibrium points and their linear stability in the CR3BP. The obtained results of this model can be applied to study the motion (locations and stability) of a test particle around the collinear points of the binary systems RXJ 0450.1-5856 and Cen X-4.

This paper is organized as follows. In sect. 2, the equations governing the motion are presented. The existence of collinear equilibrium points is discussed in sect. 3, while sect. 4 examines their linear stability of these points. Numerical analysis is done in sect. 5. Finally, sect. 6 summarizes the conclusion of our paper.

2 Equations of motion

Using a barycentric-synodic coordinate system $(x,\ y)$ and dimensionless variables, the equations of motion of a test particle in the CR3BP under the effects of oblateness of the bigger primary and the radiation of the smaller primary can be expressed as

$$\begin{aligned} \ddot{x} - 2n\dot{y} &= \Omega_x \\ \ddot{y} + 2n\dot{x} &= \Omega_y \end{aligned} \tag{1}$$

where

$$\begin{aligned} \Omega_x &= n^2 x - \frac{(1-\mu)(x+\mu)}{r_1^3} - \frac{3(1-\mu)A(x+\mu)}{2r_1^5} - \frac{\mu q(x+\mu-1)}{r_2^3}\,, \\ \Omega_y &= n^2 y - \frac{(1-\mu)y}{r_1^3} - \frac{3(1-\mu)Ay}{2r_1^5} - \frac{\mu q y}{r_2^3}\,, \\ r_1^2 &= (x+\mu)^2 + y^2, \qquad r_2^2 = (x+\mu-1)^2 + y^2, \end{aligned} \tag{2}$$

$$n^2 = 1 + \frac{3A}{2}\,. \tag{3}$$

Here r_1 and r_2 are the respective distances of the test particle from the primaries m_1 and m_2 separated by a distance R. The mean motion n of the primaries is given by $n^2 = 1 + \frac{3A}{2}$, where $0 < A = \frac{r_e^2 - r_\rho^2}{5R^2} \ll 1$ is the oblateness coefficient of m_1 having the equatorial and polar radii as r_e and r_p, respectively. $0 < \mu = \frac{m_2}{m_1+m_2} \leq \frac{1}{2}$ be the mass parameter. q characterizes the effects of radiation of the smaller primary, and is given by $0 < q = 1 - \frac{F_p}{F_g} \leq 1$, where F_p and F_g are the radiation pressure and the gravitational force, respectively.

The equations of motion are affected by the shape of the bigger primary and the radiation pressure of the smaller primary. Next, we shall discuss the positions of the collinear equilibrium points of the test particle.

3 Positions of collinear equilibrium points

The collinear equilibrium points can be obtained by solving equations $\Omega_x = 0$, $y = 0$. Therefore, we have

$$f(x) \equiv n^2 x - \frac{(1-\mu)(x+\mu)}{r_1^3} - \frac{3(1-\mu)A(x+\mu)}{2r_1^5} - \frac{\mu q(x+\mu-1)}{r_2^3} = 0, \tag{4}$$

where

$$r_1 = |x+\mu| \qquad \text{and} \qquad r_2 = |x+\mu-1|. \tag{5}$$

Computation of the position of collinear point L_1.

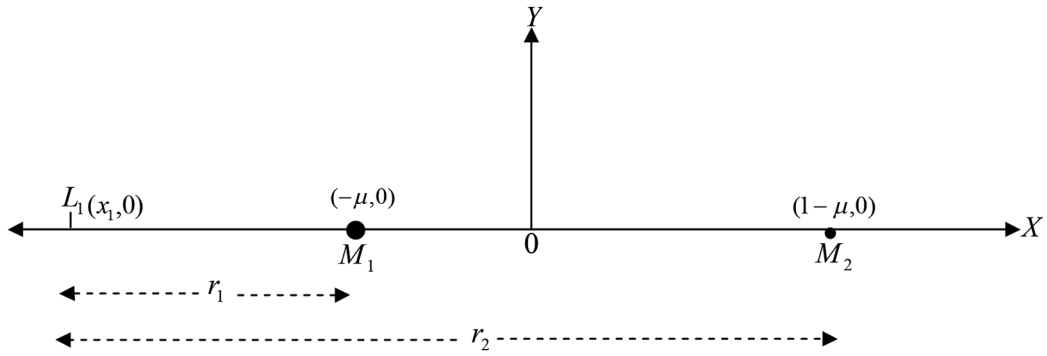

Fig. 1. Position of the collinear point L_1.

Computation of the position of collinear point L_2.

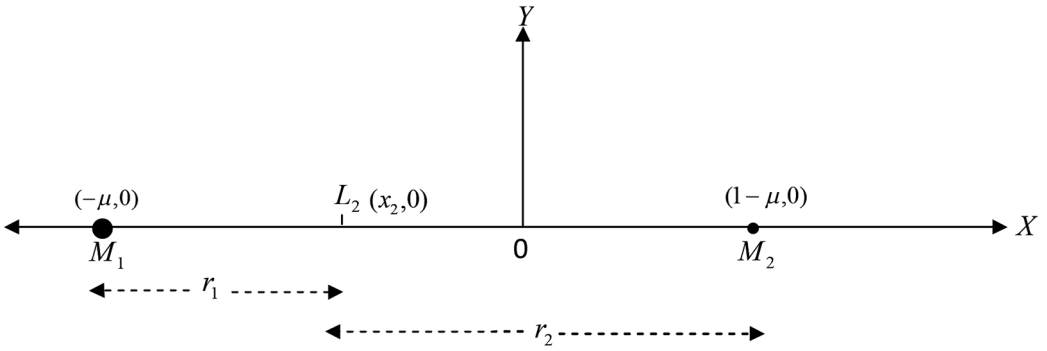

Fig. 2. Position of the collinear point L_2.

The abscissae of the collinear points are the roots of the equation $f(x) = 0$. To locate these points, we observe the behaviour of the function $f(x)$. There are only three real roots of the equation $f(x) = 0$ with one lying in each of the open interval $(-\mu - 1, -\mu)$, $(-\mu, 0)$, and $(1 - \mu, 2 - \mu)$. These roots correspond to the three collinear points and are denoted by L_1, L_2 and L_3.

Figures 1, 2 and 3 are sketches of the locations of the collinear points. In fig. 1, L_1 is located to the left of the bigger primary on the negative x-axis. Let ε_1 be the distance of L_1 from the primary m_1, so that $r_1 = \varepsilon_1$, $r_2 = 1 + \varepsilon_1$ and $x_1 = -\mu - \varepsilon_1$. Then from eqs. (4) and (5), we have

$$n^2(-\mu - \varepsilon_1) + \frac{(1-\mu)}{\varepsilon_1^2} + \frac{3(1-\mu)A}{2\varepsilon_1^4} + \frac{\mu q}{(1+\varepsilon_1)^2} = 0, \tag{6}$$

such that

$$\begin{aligned} &- n^2{\varepsilon_1}^7 - n^2(2+\mu){\varepsilon_1}^6 - n^2(1+2\mu){\varepsilon_1}^5 + \left(1 - \mu\left(1 + n^2 - q\right)\right){\varepsilon_1}^4 + 2(1-\mu){\varepsilon_1}^3 \\ &+ n^2(1-\mu){\varepsilon_1}^2 + 3A(1-\mu)\varepsilon_1 + \frac{3}{2}A(1-\mu) = 0. \end{aligned} \tag{7}$$

Equation (7) is a seventh-degree algebraic equation in ε_1:

$$n^2(-\mu - \varepsilon_1 - \mu\varepsilon_1 + \mu\varepsilon_1) + (1-\mu){\varepsilon_1}^{-2} + \frac{3}{2}(1-\mu)A{\varepsilon_1}^{-4} + \mu q(1+\varepsilon_1)^{-2} = 0.$$

Simplifying the above, we get an analogous polynomial of same degree to eq. (7) as

$${\varepsilon_1}^7 + a{\varepsilon_1}^6 + b{\varepsilon_1}^5 + c{\varepsilon_1}^4 - d{\varepsilon_1}^3 - e{\varepsilon_1}^2 - f\varepsilon_1 - g = 0, \tag{8}$$

Computation of the position of collinear point L_3.

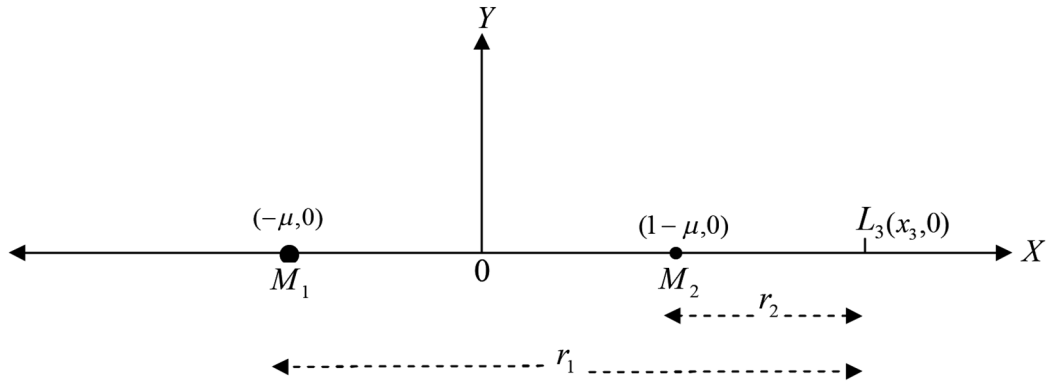

Fig. 3. Position of the collinear point L_3.

where

$$\upsilon = \frac{\mu}{(1-\mu)},$$
$$a = \left(\frac{2+3\upsilon}{1+\upsilon}\right), \qquad b = \frac{1}{1+\upsilon}(1+3\upsilon), \qquad c = \frac{1}{1+\upsilon}\left(-\frac{1}{n^2}+\upsilon-\frac{q\upsilon}{n^2}\right), \qquad d = \frac{1}{1+\upsilon}\left(\frac{2}{n^2}\right),$$
$$e = \frac{1}{1+\upsilon}\left(\frac{1}{n^2}+\frac{3}{2n^2}A\right), \qquad f = \frac{1}{1+\upsilon}\left(\frac{3}{n^2}\right)A \qquad \text{and} \qquad g = \frac{1}{1+\upsilon}\left(\frac{3}{2n^2}A\right).$$

Here, the point L_2 lies between the primaries m_1 and m_2 on the x-axis (see fig. 2). Let ε_2 be the distance of L_2 from the primary m_2, so that $r_1 = 1-\varepsilon_2$, $r_2 = \varepsilon_2$ and $x_2 = 1-\mu-\varepsilon_2$. Then from eqs. (4) and (5), we have

$$n^2(1-\mu-\varepsilon_2) - \frac{(1-\mu)}{(1-\varepsilon_2)^2} - \frac{3(1-\mu)A}{2(1-\varepsilon_2)^4} + \frac{\mu q}{{\varepsilon_2}^2} = 0, \tag{9}$$

such that

$$\begin{aligned} &-n^2{\varepsilon_2}^7 + n^2(5-\mu){\varepsilon_2}^6 - n^2(10-4\mu){\varepsilon_2}^5 + (n^2(10-6\mu)+\mu(1+q)-1){\varepsilon_2}^4 \\ &-\left(n^2(5+4\mu)+2(-1+\mu(1+2q))\right){\varepsilon_2}^3 + 6\mu q{\varepsilon_2}^2 - 4\mu q\varepsilon_2 + \mu q = 0. \end{aligned} \tag{10}$$

Equation (10) is an algebraic equation of seventh degree in ε_2:

$$n^2(1-\mu-\varepsilon_2+\mu\varepsilon_2-\mu\varepsilon_2) - (1-\mu)(1-\varepsilon_2)^{-2} - \frac{3}{2}(1-\mu)A(1-\varepsilon_2)^{-4} + \mu q{\varepsilon_2}^{-2} = 0.$$

Simplifying the above, we get an analogous polynomial of same degree to eq. (10) as

$${\varepsilon_2}^7 - a{\varepsilon_2}^6 + b{\varepsilon_2}^5 - c{\varepsilon_2}^4 + d{\varepsilon_2}^3 - e{\varepsilon_2}^2 + f\varepsilon_2 - g = 0, \tag{11}$$

where

$$\upsilon = \frac{\mu}{(1-\mu)},$$
$$a = \frac{1}{1+\upsilon}(5+4\upsilon), \qquad b = \frac{1}{1+\upsilon}(10+6\upsilon), \qquad c = \frac{1}{1+\upsilon}\left(-\frac{1}{n^2}+10+\frac{q\upsilon}{n^2}+4\upsilon\right),$$
$$d = \frac{1}{1+\upsilon}\left(-\frac{2}{n^2}+5+\frac{4q\upsilon}{n^2}+\upsilon\right), \qquad e = \frac{1}{1+\upsilon}\left(-\frac{1}{n^2}+1+\frac{6q\upsilon}{n^2}-\frac{3}{2n^2}A\right),$$
$$f = \frac{1}{(1+\upsilon)n^2}(4q\upsilon) \qquad \text{and} \qquad g = \frac{q\upsilon}{(1+\upsilon)n^2}.$$

Table 1. Numerical data for binary systems.

Binary	Mass ratio	Radiation pressure		
	μ	q	M_1	M_2
RXJ 0450.1-5856	0.0967	0.9965	1.4	0.15
Cen X-4	0.038515	0.993	1.9996	0.0801

In this case, L_3 is located to the right of the radiating smaller primary on the positive x-axis (see fig. 3). Let ε_3 be the distance of L_3 from the primary m_2, so that $r_1 = 1+\varepsilon_3$, $r_2 = \varepsilon_3$ and $x_3 = 1-\mu+\varepsilon_3$. Then from eqs. (4) and (5), we have

$$n^2(1-\mu+\varepsilon_3) - \frac{(1-\mu)}{(1+\varepsilon_3)^2} - \frac{3(1-\mu)A}{2(1+\varepsilon_3)^4} - \frac{\mu q}{{\varepsilon_3}^2} = 0, \tag{12}$$

such that

$$\begin{aligned} &n^2{\varepsilon_3}^7 + n^2(5-\mu){\varepsilon_3}^6 + n^2(10-4\mu){\varepsilon_3}^5 + \left(n^2(10-6\mu)+\mu(1-q)-1\right){\varepsilon_3}^4 \\ &+ \left(n^2(5-4\mu) - 2(1-\mu(1-2q))\right){\varepsilon_3}^3 - 6\mu q{\varepsilon_3}^2 - 4\mu q\varepsilon_3 - \mu q = 0. \end{aligned} \tag{13}$$

Equation (13) is an algebraic equation of seventh degree in ε_3:

$$n^2(1-\mu+\varepsilon_3-\mu\varepsilon_3+\mu\varepsilon_3) - (1-\mu)(1+\varepsilon_3)^{-2} - \frac{3}{2}(1-\mu)A(1+\varepsilon_3)^{-4} - \mu q{\varepsilon_3}^{-2} = 0.$$

Simplifying the above, we get an analogous polynomial of same degree to eq. (13) as

$${\varepsilon_3}^7 + a{\varepsilon_3}^6 + b{\varepsilon_3}^5 + c{\varepsilon_3}^4 + d{\varepsilon_3}^3 - e{\varepsilon_3}^2 - f\varepsilon_3 - g = 0, \tag{14}$$

where

$$\begin{aligned} &\upsilon = \frac{\mu}{(1-\mu)}, \\ &a = \frac{(5+4\upsilon)}{1+\upsilon}, \qquad b = \frac{(10+6\upsilon)}{1+\upsilon}, \qquad c = \frac{1}{1+\upsilon}\left(10 - \frac{1}{n^2} + 4\upsilon - \frac{q\upsilon}{n^2}\right), \\ &d = \frac{1}{1+\upsilon}\left(5 - \frac{2}{n^2} + \upsilon - \frac{4q\upsilon}{n^2}\right), \qquad e = \frac{1}{1+\upsilon}\left(1 - \frac{1}{n^2} - \frac{6q\upsilon}{n^2} - \frac{3}{2n^2}A\right), \\ &f = \frac{4q\upsilon}{n^2(1+\upsilon)} \qquad \text{and} \qquad g = \frac{q\upsilon}{n^2(1+\upsilon)}. \end{aligned}$$

Using the software *Mathematica*, and taking the value of the oblateness coefficient $A = 0.2$, we obtain the numerical solutions of eqs. (8), (11) and (14) for the binary systems RXJ 0450.1-5856 and Cen X-4. The bigger primary is a stellar remnant (a neutron star) and the smaller one, a low mass stellar companion. The obtained solutions for these systems are $\varepsilon_1 = 0.949633$, $\varepsilon_2 = 0.246854$, $\varepsilon_3 = 0.315041$, and $\varepsilon_1 = 0.979900$, $\varepsilon_2 = 0.186277$, $\varepsilon_3 = 0.223103$, respectively. Then, from $x_1 = -\mu-\varepsilon_1$, $x_2 = 1-\mu-\varepsilon_2$ and $x_3 = 1-\mu+\varepsilon_3$, we list the x-coordinates of the collinear equilibria L_1, L_2, and L_3 in tables 2 and 3. Figures 4–9 are surface representations of the positions of collinear points, and have been plotted for (A, q, L_1); (A, q, L_2) and (A, q, L_3), axes, respectively, for various assumed values of oblateness of the bigger primary, and radiation pressure force of the smaller primary for the binary systems RXJ 0450.1-5856 and Cen X-4. The numerical data for the binaries are given in table 1, where the radiation pressure q is obtained from [45].

Tables 2 and 3 show the effect of oblateness on the collinear points of RXJ 0450.1-5856 and Cen X-4, respectively. In each system /case, we first compute the position of the collinear points in the absence of oblateness and radiation pressure (classical) and then for the binaries, with an assumed small oblateness. The summary effect is a shift nearer to or away from the primaries depending on the system parameters.

4 Stability of collinear equilibrium points

We now examine the stability of an equilibrium configuration, that is, its ability to restrain the body motion in its vicinity. To do so, we displace the third body a little from an equilibrium point with a small velocity. If its motion is a rapid departure from the vicinity of the point, we call such a position an unstable one. However, if the body merely oscillates about the point, it is said to be a stable position. Let the location of an equilibrium point be denoted by (a_0, b_0) and consider a small displacement (ξ, η) from the point such that $x = a_0 + \xi$ and $y = b_0 + \eta$. Substituting these values in (1), we obtain the variational equations.

Table 2. Computations of the collinear equilibrium points for varying oblateness and radiation for RXJ 0450.1-5856.

Cases	A	q	xL_1	xL_2	xL_3
1	0	1	−1.04024	0.615350	1.25846
		0.9965	−1.04021	0.615640	1.25802
2	0.0001	1	−1.04024	0.615381	1.25844
		0.9965	−1.04022	0.615671	1.25800
3	0.001	1	−1.04029	0.615657	1.25822
		0.9965	−1.04026	0.615947	1.25777
4	0.002	1	−1.04033	0.615963	1.25797
		0.9965	−1.04030	0.616252	1.25753
5	0.01	1	−1.04070	0.618347	1.25604
		0.9965	−1.04067	0.618632	1.25559
6	0.02	1	−1.04113	0.621183	1.25366
		0.9965	−1.04110	0.621466	1.25322
7	0.03	1	−1.04154	0.623876	1.25135
		0.9965	−1.04152	0.624155	1.25091
8	0.05	1	−1.04231	0.628884	1.24687
		0.9965	−1.04228	0.629157	1.24644
9	0.1	1	−1.04394	0.639655	1.23652
		0.9965	−1.04392	0.639915	1.23610
10	0.2	1	−1.04635	0.656203	1.21874
		0.9965	−1.04633	0.656446	1.21834

Table 3. Computations of the collinear equilibrium points for varying oblateness and radiation for Cen X-4.

Cases	A	q	xL_1	xL_2	xL_3
1	0	1	−1.01604	0.744951	1.21443
		0.993	−1.01602	0.745409	1.21380
2	0.0001	1	−1.01605	0.744973	1.21441
		0.993	−1.01602	0.745431	1.21379
3	0.001	1	−1.01606	0.745166	1.21425
		0.993	−1.01604	0.745624	1.21362
4	0.002	1	−1.01608	0.745380	1.21406
		0.993	−1.01606	0.745870	1.21344
5	0.01	1	−1.01622	0.747054	1.21262
		0.993	−1.01620	0.747507	1.21200
6	0.02	1	−1.01639	0.749060	1.21085
		0.993	−1.01637	0.749508	1.21023
7	0.03	1	−1.01655	0.750979	1.20913
		0.993	−1.01653	0.751422	1.20852
8	0.05	1	−1.01684	0.754580	1.20581
		0.993	−1.01682	0.755014	1.20520
9	0.1	1	−1.01748	0.762454	1.19817
		0.993	−1.01746	0.762870	1.19758
10	0.2	1	−1.01843	0.774819	1.18515
		0.993	−1.01842	0.775208	1.18459

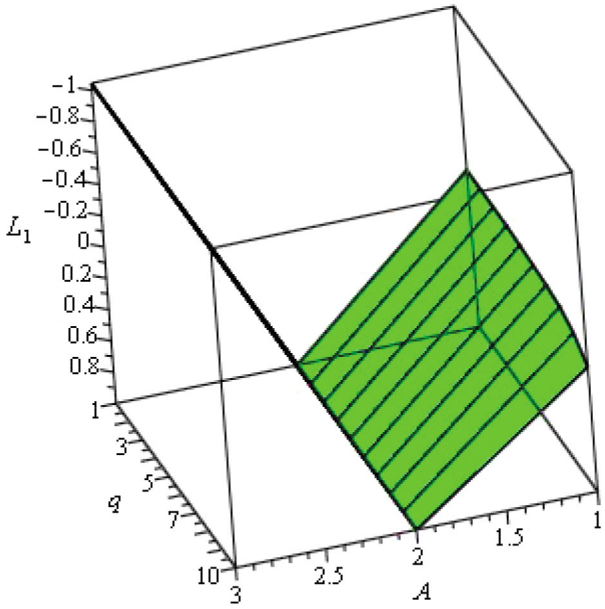

Fig. 4. Effect of oblateness on the collinear point L_1 of RXJ 0450.1-5856.

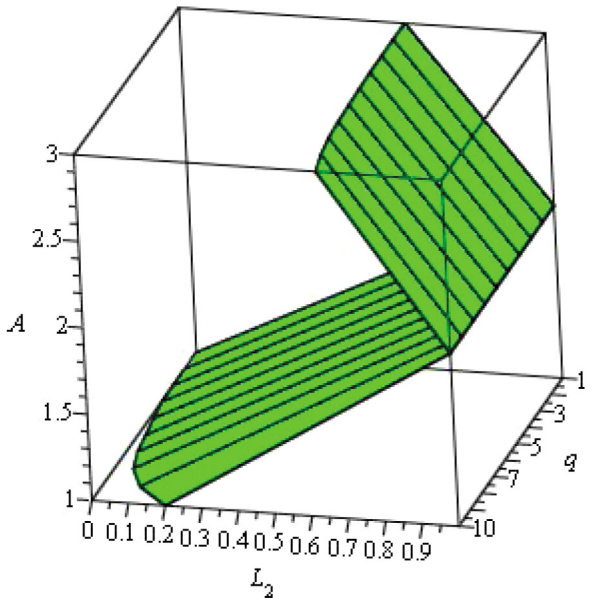

Fig. 5. Effect of oblateness on the collinear point L_2 of RXJ 0450.1-5856.

To study the stability of collinear equilibrium points, we obtain the variational equations of motion as

$$\ddot{\xi} - 2n\dot{\eta} = \xi(\Omega_{xx})^0 + \eta(\Omega_{xy})^0,$$
$$\ddot{\eta} + 2n\dot{\xi} = \xi(\Omega_{xy})^0 + \eta(\Omega_{yy})^0. \tag{15}$$

Here, only linear terms in ξ and η have been taken. The second partial derivatives of Ω are denoted by subscripts. We get the corresponding characteristics equation:

$$\lambda^4 - (\Omega^0_{xx} + \Omega^0_{yy} - 4n^2)\lambda^2 + \Omega^0_{xx}\Omega^0_{yy} - (\Omega^0_{xy})^2 = 0, \tag{16}$$

where the superscripts 0 indicate that the partial derivatives have been calculated at the collinear equilibrium point under investigation.

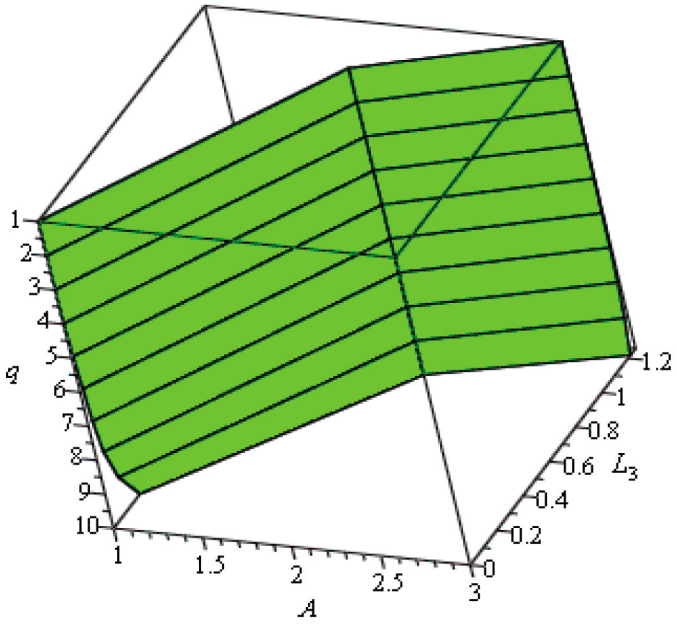

Fig. 6. Effect of oblateness on the collinear pointL_3 of RXJ 0450.1-5856.

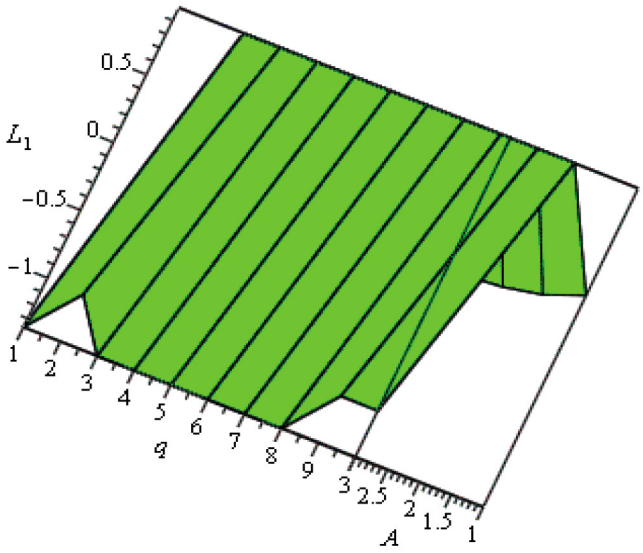

Fig. 7. Effect of oblateness on the collinear pointL_1 of Cen X-4.

Clearly, from eq. (1), we get the equations

$$\Omega_x = n^2 x - \frac{(1-\mu)(x+\mu)}{r_1^3} - \frac{3(1-\mu)A(x+\mu)}{2r_1^5} - \frac{\mu q(x+\mu-1)}{r_2^3}\,, \tag{17}$$

$$\Omega_y = n^2 y - \frac{(1-\mu)y}{r_1^3} - \frac{3(1-\mu)Ay}{2r_1^5} - \frac{\mu q y}{r_2^3}\,, \tag{18}$$

where $r_1^2 = (x+\mu)^2 + y^2$, $r_2^2 = (x+\mu-1)^2 + y^2$.

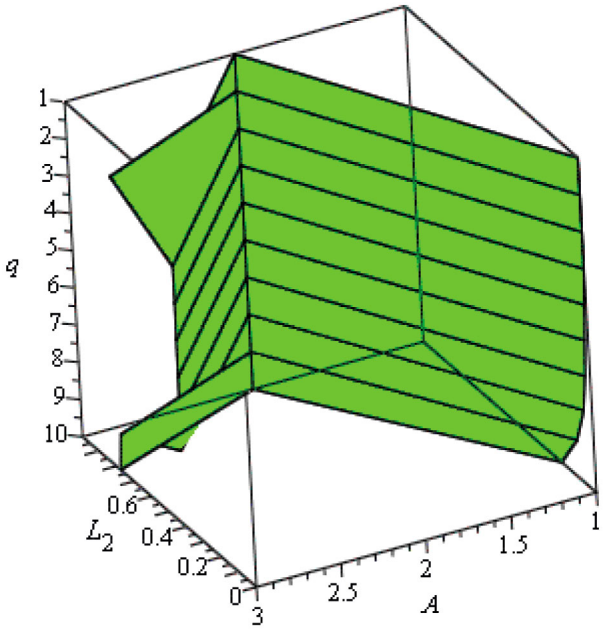

Fig. 8. Effect of oblateness on the collinear point L_2 of Cen X-4.

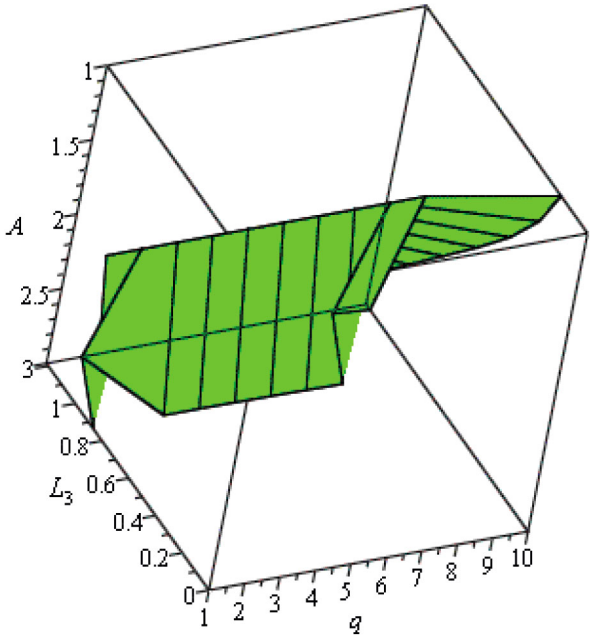

Fig. 9. Effect of oblateness on the collinear point L_3 of Cen X-4.

Therefore, from eqs. (17) and (18), we obtain

$$\Omega_{xx} = n^2 - \frac{(1-\mu)}{r_1^3} + \frac{3(1-\mu)(x+\mu)^2}{r_1^5} - \frac{3(1-\mu)A}{2r_1^5} + \frac{15(1-\mu)A(x+\mu)^2}{2r_1^7} - \frac{\mu q}{r_2^3} + \frac{3\mu q(x+\mu-1)^2}{r_2^5}, \tag{19}$$

$$\Omega_{yy} = n^2 - \frac{(1-\mu)}{r_1^3} + \frac{3(1-\mu)y^2}{r_1^5} - \frac{3(1-\mu)A}{2r_1^5} + \frac{15(1-\mu)Ay^2}{2r_1^7} - \frac{\mu q}{r_2^3} + \frac{3\mu q y^2}{r_2^5}, \tag{20}$$

$$\Omega_{xy} = \Omega_{yx} = \frac{3(1-\mu)(x+\mu)y}{r_1^5} + \frac{15(1-\mu)(x+\mu)Ay}{2r_1^7} + \frac{3\mu q(x+\mu-1)y}{r_2^5}. \tag{21}$$

In the case of the collinear point L_2 lying on the x-axis between the primaries. We have $r_1 = 1-\varepsilon_2$, $r_2 = \varepsilon_2$ such that $x_0 = 1-\mu-\varepsilon_2$, where ε_2 is the distance of L_2 from the smaller primary.

Now, substituting $x_0 = 1-\mu-\varepsilon_2$ in eq. (19) to get

$$\Omega^0_{xx} = n^2 - \frac{(1-\mu)}{|x_0+\mu|^3} + \frac{3(1-\mu)(x_0+\mu)^2}{|x_0+\mu|^5} - \frac{3(1-\mu)A}{2|x_0+\mu|^5} + \frac{15(1-\mu)A(x_0+\mu)^2}{2|x_0+\mu|^7} - \frac{\mu q}{|x_0+\mu-1|^3} + \frac{3\mu q(x_0+\mu-1)^2}{|x_0+\mu-1|^5},$$

$$\Omega^0_{xx} = n^2 + \frac{2(1-\mu)}{(1-\varepsilon_2)^3} + \frac{6(1-\mu)A}{(1-\varepsilon_2)^5} + \frac{2\mu q}{(\varepsilon_2)^3} > 0. \tag{22}$$

Similarly, from eq. (20), on substituting $x_0 = 1-\mu-\varepsilon_2$,

$$\Omega^0_{yy} = n^2 - \frac{(1-\mu)}{r_1^3} - \frac{3(1-\mu)A}{2r_1^5} - \frac{\mu q}{r_2^3},$$

$$\Omega^0_{yy} = n^2 - \left[\frac{(1-\mu)}{(1-\varepsilon_2)^3} + \frac{3(1-\mu)A}{2(1-\varepsilon_2)^5} + \frac{\mu q}{(\varepsilon_2)^3}\right] < 0. \tag{23}$$

Lastly, from eq. (21), on putting $y = 0$ we have

$$\Omega^0_{xy} = \Omega^0_{yx} = 0. \tag{24}$$

Now, since $\varepsilon_i > 0$ $(i = 1, 2, 3)$, $(1-q) \ll 1$, $0 < \mu \leq \frac{1}{2}$ and $A \ll 1$. We have $\Omega^0_{xx} > 0$, $\Omega^0_{yy} < 0$, and $\Omega^0_{xy} = 0$.

Since $\Omega^0_{xx}\Omega^0_{yy} < 0$, this implies that the discriminant of (16) will be positive and the roots can be expressed as $\lambda_1 = s_1$, $\lambda_2 = -s_1$, $\lambda_3 = is_2$, and $\lambda_4 = -is_2$ where $s_i (i = 1, 2)$ are real. Therefore, the motion around the collinear point L_2 is unstable. The same stability analysis can be done for the collinear equilibrium points L_1 and L_3. Hence, these points remain unstable as the classical restricted three-body problem [16].

We have seen that the collinear points are, in general, unstable; but by assigning the appropriate initial conditions for the disturbed motion around theses points, they can be made points of stability. The orbits of the infinitesimal mass around these points are ellipse, which are parallel to the x- and y-axes of the rotating coordinate system. However, the motion is retrograde along the orbits. These features are used in planning a mission around the collinear points.

For the further numerical investigation, we simplify the characteristic equation (16) using eqs. (22), (23) and (24). The characteristic equation reduces to

$$\lambda^4 - \left[n^2 + \frac{2(1-\mu)}{(1-\varepsilon_2)^3} + \frac{6(1-\mu)A}{(1-\varepsilon_2)^5} + \frac{2\mu q}{(\varepsilon_2)^3} + n^2 - \frac{(1-\mu)}{(1-\varepsilon_2)^3} - \frac{3(1-\mu)A}{2(1-\varepsilon_2)^5} - \frac{\mu q}{(\varepsilon_2)^3} - 4n^2\right]\lambda^2$$
$$+ \left(n^2 + \frac{2(1-\mu)}{(1-\varepsilon_2)^3} + \frac{6(1-\mu)A}{(1-\varepsilon_2)^5} + \frac{2\mu q}{(\varepsilon_2)^3}\right)\left(n^2 - \frac{(1-\mu)}{(1-\varepsilon_2)^3} - \frac{3(1-\mu)A}{2(1-\varepsilon_2)^5} - \frac{\mu q}{(\varepsilon_2)^3}\right) = 0, \tag{25}$$

such that

$$\lambda^4 + [P]\lambda^2 + R = 0, \tag{26}$$

where

$$P = 2 + 3A - \frac{(1-\mu)}{(1-\varepsilon_2)^3} - \frac{9(1-\mu)A}{2(1-\varepsilon_2)^5} - \frac{\mu q}{(\varepsilon_2)^3}.$$

$$R = 1 + 3A + \frac{(1-\mu)}{(1-\varepsilon_2)^3} + \frac{3A(1-\mu)}{(1-\varepsilon_2)^3} - \frac{2(\mu q)^2}{(\varepsilon_2)^6} + \frac{9(1-\mu)A}{2(1-\varepsilon_2)^5} + \frac{\mu q}{(\varepsilon_2)^3} + \frac{3A\mu q}{(\varepsilon_2)^3} - \frac{2(1-\mu)^2}{(1-\varepsilon_2)^6} - \frac{9(1-\mu)^2 A}{(1-\varepsilon_2)^8}$$
$$- \frac{4\mu q(1-\mu)}{(\varepsilon_2)^3(1-\varepsilon_2)^3} - \frac{9\mu q(1-\mu)A}{(\varepsilon_2)^3(1-\varepsilon_2)^5}.$$

5 Numerical applications

We numerically investigate the stability of the collinear equilibrium points for the binary systems RXJ 0450.1-5856 and Cen X-4 using the software package *Mathematica* in eq. (26). For this, we compute the characteristic roots for varying parameters, and list them in tables 4 and 5, respectively.

Tables 4 and 5 show the characteristic roots to be negative, positive or complex. We conclude that the collinear equilibrium points are unstable due to the presence of positive roots and positive real parts in the complex roots [16]. Our results agree with previous assertions of [27,45].

Table 4. Roots of the characteristic equation (26), for the binary system RXJ 0450.1-5856.

A	ε_1	$\lambda_{1,2}$	$\lambda_{3,4}$	ε_2	$\lambda_{1,2}$	$\lambda_{3,4}$	ε_3	$\lambda_{1,2}$	$\lambda_{3,4}$
0	0.943511	±2046.7	±0.70.7819 i	0.287660	±3.37691	±0.2.61845 i	0.35472	±6.54158	±0.2.21429 i
0.0001	0.943516	±2125.89	±0.72.4367 i	0.287629	±3.37759	±0.2.61877 i	0.354695	±6.54281	±0.2.21455 i
0.001	0.943558	±2740.41	±0.85.9537 i	0.287353	±3.38363	±0.2.62161 i	0.354475	±6.55396	±0.2.21686 i
0.002	0.943605	±3296.98	±0.98.9231 i	0.287048	±3.39032	±0.2.62477 i	0.35423	±6.56621	±0.2.21942 i
0.01	0.943969	±6257.9	±0.172.246 i	0.284668	±3.44284	±0.2.64974 i	0.352293	±6.66072	±0.2.23961 i
0.02	0.944404	±8837.63	±0.237.223 i	0.281834	±3.50614	±0.2.68035 i	0.349924	±6.77057	±0.2.26419 i
0.03	0.944817	±11003.4	±0.291.222 i	0.279145	±3.56705	±0.2.71030 i	0.34761	±6.87217	±0.2.28809 i
0.05	0.945584	±14809.0	±0.384.182 i	0.274143	±3.68266	±0.2.76843 i	0.34314	±7.05417	±0.2.33399 i
0.1	0.947217	±23197.3	±0.580.393 i	0.263385	±3.94288	±0.2.90483 i	0.332796	±7.41528	±0.2.43943 i
0.2	0.949633	±38635.1	±0.918.205 i	0.246854	±4.38054	±0.3.14863 i	0.315041	±7.89591	±0.2.62172 i

Table 5. Roots of the characteristic equation (26), for the binary system Cen X-4.

A	ε_1	$\lambda_{1,2}$	$\lambda_{3,4}$	ε_2	$\lambda_{1,2}$	$\lambda_{3,4}$	ε_3	$\lambda_{1,2}$	$\lambda_{3,4}$
0	0.977507	±21877.4	±0.290.668 i	0.216076	±3.14313	±0.2.46828 i	0.252319	±4.41112	±0.2.07787 i
0.0001	0.977509	±26748.8	±0.331.015 i	0.216054	±3.14371	±0.2.46858 i	0.252301	±4.41209	±0.2.07791 i
0.001	0.977525	±53470.8	±0.579.819 i	0.215861	±3.14878	±0.2.47117 i	0.252136	±4.41780	±0.2.07996 i
0.002	0.977543	±72571.2	±0.768.057 i	0.215648	±3.15440	±0.2.47404 i	0.251954	±4.42446	±0.2.08204 i
0.01	0.977684	±159699.	±0.1640.85 i	0.213978	±3.19876	±0.2.49686 i	0.250511	±4.47651	±0.2.09864 i
0.02	0.977852	±230790.	±0.2345.4 i	0.211977	±3.25271	±0.2.52493 i	0.248749	±4.53888	±0.2.11915 i
0.03	0.978012	±289488.	±0.2916.98 i	0.210063	±3.30515	±0.2.55254 i	0.247031	±4.59850	±0.2.13942 i
0.05	0.978310	±391606.	±0.3887.86 i	0.206471	±3.40593	±0.2.60642 i	0.243719	±4.71040	±0.2.17925 i
0.1	0.978948	±614609.	±0.5914.58 i	0.198615	±3.63803	±0.2.73435 i	0.236090	±4.95569	±0.2.27499 i
0.2	0.979900	±1022510.	±0.9382.83 i	0.186277	±4.04100	±0.2.96693 i	0.223103	±5.34763	±0.2.45265 i

6 Discussion and conclusion

The existence and linear stability of the collinear equilibrium points, under the joint effects of oblateness of the bigger primary, and radiation of the smaller primary have been studied. The equations of motion are affected by the radiation of the smaller primary and the oblateness of the bigger primary. The equations of motion (1) are analogous but not exact to those of [46] and [45]. If $y = 0$, eqs. (4) and (5) determine the positions of the collinear equilibrium points of the infinitesimal body, and they locate the three points L_1, L_2 and L_3 forming horizontally with the line joining the primaries. It is noted that, the radiating primary produces this shift away from itself, while the oblate one is toward others.

The stability of the collinear equilibrium points is determined by the roots of the characteristic equation (26). We investigate the stability of the systems using a numerical approach and reveal the existence of at least a positive root and/or a positive real part. Consequently, the motion is unbounded, and thus unstable. Our results in the circular case agree with those of [27,45]. In all these communications however, the stability analysis remains the same, collinear equilibria remain unstable.

References

1. A.D. Bruno, *The restricted three-body problem: periodic orbits* (De Gruyter, 1994).
2. M. Gutzwiller, Rev. Mod. Phys. **15**, 46 (1998).
3. F. Topputo, M. Vasile, F. Bernilli-Zazzara, Ann. N. Y. Acad. Sci. **1065**, 55 (2005).
4. M. Valtonen, H. Karttunen, *The Three-Body Problem* (Cambridge University Press, 2006).
5. A. Chenciner, Scholarpedia **2**, 2111 (2007).
6. E. Belbruno, F. Topputo, M. Gidea, Adv. Space Res. **42**, 1330 (2008).
7. D. Romagnoli, C. Circi, Celest. Mech. Dyn. Astron. **103**, 79 (2009).
8. A. Farres, A. Jorba, Acta Astron. **63**, 249 (2010).
9. A. Bazso, *Lunar effects on close encounters of near earth asteroids*, in *43rd Lunar and Planetary Science Conference* (Lunar and Planetary Institute, 2012).
10. S. Bucciarelli, M. Ceccaroni, A. Celletti, G. Pucacco, Ann. Mat. Pura Appl. **195**, 489 (2016) doi: 10.1007/s10231-015-0474-2.
11. L. Euler, Nov. Comm. Petrop. **11**, 144 (1797).
12. J. Langrange, *Essai d'une nouvelle méthode pour résoudre le problème des trois corps*, Vol. **9** (Panekoucke, Paris, 1772).
13. Ch. Delaunay, Mem. Acad. Sci. **28**, 29 (1867).
14. H. Poincaré, *Les Méthodes Nouevelles de la Méchanique céleste* (Guthier Villars, Paris, 1842) pp. 250, Chap. V.
15. G.D. Birkhoff, *Dynamical System* (American Mathematics Society, New York, 1927).
16. V. Szebehely, *Theory of orbits. The restricted problem of three bodies* (Academic Press, New York, 1967).
17. J.M.A. Danby, *Fundamentals of Celestial Mechanics*, second edition (Willmann-Bell Inc., Virginia, 1988).
18. A.L. Kunitsyn, A.T. Tureshbaev, Pis'ma Astron. Zh. **9**, 432 (1983).
19. S.N. Khasan, Cosmic Res. **34**, 504 (1996).
20. S.K. Sahoo, B. Ishwar, Bull. Astron. Soc. India **28**, 579 (2000).
21. A.L. Kunitsyn, J. Appl. Math. Mech. **64**, 757 (2000).
22. A.S. Zimovshchikov, V.N. Tkhai, J. Appl. Math. Mech. **74**, 158 (2010).
23. N.V. Tkhai, J. Appl. Math. Mech. **76**, 441 (2012).
24. E.I. Abouelmagd, S.M. El-Shaboury, Astrophys. Space Sci. **341**, 331 (2012).
25. E.I. Abouelmagd, Astrophys. Space Sci. **346**, 51 (2013).
26. M. Ceccaroni, A. Celletti, G. Pucacco, Int. J. Non-Linear Mech. **81**, 65 (2016).
27. J. Singh, A. Umar, New Astron. **29**, 36 (2014).
28. M. Ceccaroni, A. Celletti, G. Pucacco, Physica D **317**, 28 (2016).
29. V.V. Radzievsky, Astrophys. J. **27**, 249 (1950).
30. D.P. Hamilton, J.A. Burns, Icarus **96**, 43 (1992).
31. J. Singh, B. Ishwar, Bull. Astron. Soc. India **27**, 415 (1999).
32. A. Farres, A. Jorba, Cel. Mech. Dyn. Astron. **107**, 233 (2008).
33. J. Singh, Astron. J. **137**, 3286 (2009).
34. J. Singh, O. Leke, U. Aishetu, Astrophys. Space Sci. **32**, 299 (2010).
35. E.I. Abouelmagd, Earth Moon Planet **110**, 143 (2013).
36. J.K. Beatty, C.C. Petersen, A. Chaikin, *The New Solar System*, 4th edition (Cambridge Universty Press, Cambridge, 1999).
37. Y.J. Du, R.X. Xu, G.J. Qiao, H.L. Han, Mon. Not. R. Astron. Soc. **399**, 1587 (2009).
38. J.W.T. Hessels, S.M. Ranson, H.I. Stairs, Space Sci. **311**, 1901 (2006).
39. P.V. SubbaRao, R.K. Sharma, Astron. Astrophys. **43**, 381 (1975).
40. A. Elipe, S. Ferrer, Cel. Mech. **37**, 59 (1985).
41. R.K. Sharma, Z.A. Taqvi, K.B. Bhatnagar, Cel. Mech. Dyn. Astron. **79**, 119 (2001).
42. C.N. Douskos, V.V. Markellos, Astron. Astrophys. **466**, 357 (2006).
43. J. Singh, T.O. Amuda, Astrophys. Space Sci. **350**, 119 (2014).
44. N. Langer, S.-C. Yoon, S. Wellstein, S. Scheithauer, ASP Conf. Ser. **261**, 252 (2002).
45. J. Singh, A. Umar, Astron. J. **143**, 109 (2013).
46. S. Kumar, B. Ishwar, Int. J. Eng. Sci. Technol. **3**, 157 (2011).